Editors' Suggestion

Fault-tolerant qubit encoding using a spin-7/2 qudit

Sumin Lim, Junjie Liu, and Arzhang Ardavan
CAESR, Department of Physics, University of Oxford, The Clarendon Laboratory, Parks Road, Oxford OX1 3PU, United Kingdom

(Received 25 May 2023; accepted 7 November 2023; published 4 December 2023)

The implementation of error correction protocols is a central challenge in the development of practical quantum information technologies. Recently, multilevel quantum resources such as harmonic oscillators and qudits have attracted interest in this context because they offer the possibility of additional Hilbert space dimensions in a spatially compact way. Here, we propose a quantum memory, implemented on a spin-7/2 nucleus hyperfine coupled to an electron spin-1/2 qubit, which provides first-order X, Y, and Z error correction using significantly fewer quantum resources than the equivalently effective qubit-based protocols. Our encoding may be efficiently implemented in existing experimentally realized molecular electron-nuclear quantum spin systems. The strategy can be extended to higher-order error protection on higher-spin nuclei.

DOI: 10.1103/PhysRevA.108.062403

On the path towards a universal quantum computer, there is a broad consensus that we are now in the noisy-intermediate-scale-quantum (NISQ) era [1]. Although some reports [2,3] suggest that quantum supremacy is possible even with NISQ devices, we are currently limited to certain specific tasks and to computations on the scale of tens of qubits. Progress beyond this will depend on the development of reliable quantum error correction strategies [4–6], because the major limitation to scalability is the rapid drop in fidelity owing to environmental noise as the system grows.

A qubit-based quantum error correction algorithm employs additional physical qubits to encode logical qubits [7–9] by providing redundancy in the Hilbert space to protect the information. Although this approach has the advantage of being mathematically compact [10] (which means it is scalable), its implementation in real systems poses challenges arising from the inherent proliferation of quantum resources required. Thus, in the current NISQ era, the traditional error-correction approach offers the dilemma of adding noisy qubits to the quantum system in an attempt to reduce noise.

This highlights the imperative of identifying hardware-efficient implementations in which error correction can be incorporated with minimal quantum resource requirements. In this context error correction algorithms exploiting not only qubits but also qudits (physical systems each offering a d-dimensional Hilbert space, with $d > 2$ in general) have attracted attention in recent years.

Among the best known is the Gottesman-Kitaev-Preskill (GKP) code and its expansion [11–13]. These proposals explore physical systems described by the quantum harmonic oscillator because, in principle, it can provide an infinite-dimensional bosonic Hilbert space for information encoding. Implementations can be provided by systems such as trapped ions or superconducting circuits [14,15]. Indeed, some experiments [16,17] have already shown enhanced coherence times for quantum states. Various theoretical programs [18,19] to generalize bosonic error correction codes are in progress.

A similar but alternative approach is to use a spin qudit, which can provide an intrinsically bounded d-level system. Qudits may be realized, for example, by electronic and nuclear spins in the solid state. Although spin-based quantum computing (specifically, exploiting ensembles of molecules whose nuclear spins were driven and detected using nuclear magnetic resonance) attracted attention and yielded some milestone experimental results in the early days of the field [20–23], intrinsic limitations on scalability were quickly identified [24]. However, recent remarkable progress on studies related to molecular magnets encourages us to explore these ingredients as basic building blocks for quantum information processing [25–29].

The size, number of spins, and basic Hamiltonian parameters for molecular magnets can be carefully tuned by chemical engineering, for example, by the selection from various options for ligand cages of a choice of magnetic ions. Furthermore, strategies for single-qudit-molecule addressing are active areas of research. For example, by analogy with the single electron transistor quantum dot, control and readout of a molecular nuclear spin in a single-molecule transistor has been reported [30,31]. Electrical control of spin—which is essential for fast manipulation and spatially localized control—is also being studied by various research groups [32–34]. The fact that spin is a basic quantum property of matter which is often only weakly coupled to other degrees of freedom suggests that may be a useful and error-robust embodiment for encoding quantum information.

In this context, we propose a strategy for constructing compact and hardware-efficient information encoding in a single spin qudit. As with the GKP code, it can provide Nth-order error correction in a Hilbert space with dimension of order N^2, which is significantly smaller than the $\sim\exp(N)$ scaling for

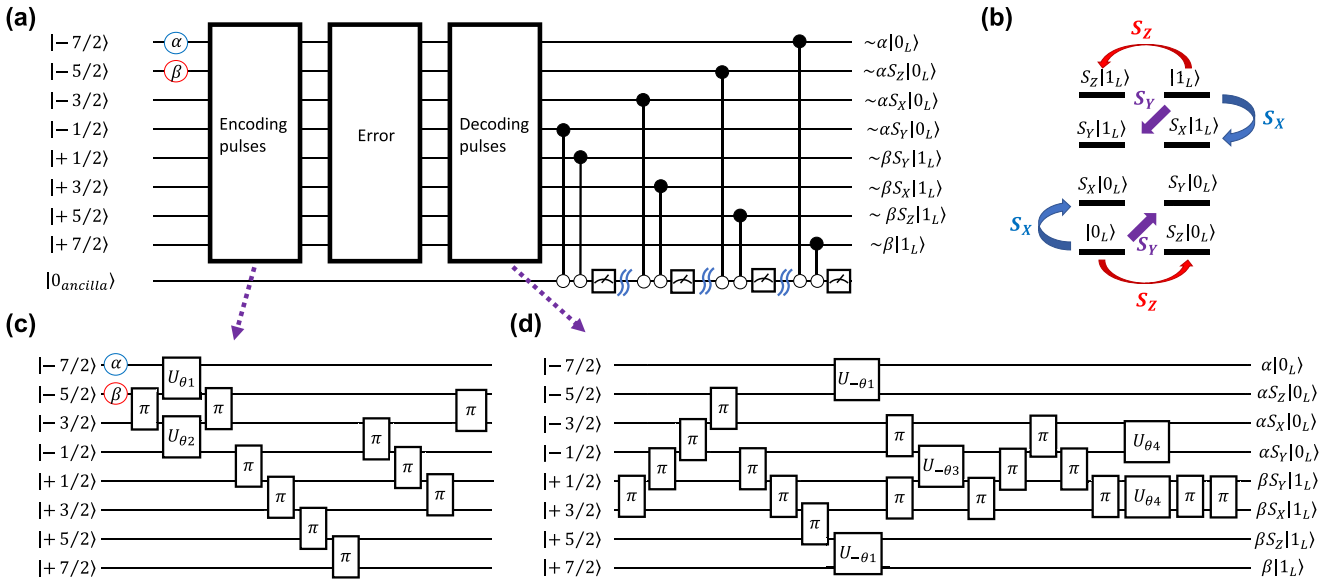

FIG. 1. A brief schematic of (a) the entire quantum error correction code, (b) the code word with first-order error, (c) the encoding pulse sequence U_{enc}, and (d) decoding pulse sequence U_{dec}. Unitary rotations U_{θ_i} are around the y axis, with $\cos\theta_i = \sqrt{3/10}, \sqrt{7/10}, \sqrt{1/5}, \sqrt{1/2}$ for $i = 1, 2, 3, 4$, respectively.

qubit implementations. However, while the GKP code is implemented on a finite subspace of an infinite-dimensional space, this encoding targets a finite-dimensional space, and we find that we need a volume half as big as for GKP. Previous reports have proposed spin qudit quantum error correction (QEC) algorithms for correcting phase errors [35–37], or logical code words to correct first-order rotation errors using one large spin [38]. In this article, we adapt a proposed encoding [38] to describe a practical implementation yielding full first-order error correction based on an electron spin qubit and a hyperfine-coupled nuclear spin-7/2, addressing the required hardware-level implementation operations, the gain offered by the protocol, and the required experimental operation fidelities. We offer a generalization to higher-order correction cases, with example code words.

Our protocol can be implemented directly in a quantum processor based on nuclear spins in the solid state (including, for example, spin-7/2 nuclei such as ^{51}V, ^{165}Ho, or ^{123}Sb) [34,39,40]. Since, among spin-qubit candidates, nuclear spins usually exhibit superior coherence times, they have already been explored as quantum information storage units in many pivotal proposals, such as Kane's early model using phosphorus donors in silicon [41], nitrogen vacancy centers in diamond [42], or hybrid structures incorporating electrical circuits and molecular magnets [31,43].

The protocol relies on projective measurement of the nuclear spin state. From a practical perspective, in the solid state this is typically achieved via measurement of a coupled electronic spin. We therefore base our proposal on an electronic spin-1/2 (acting as the ancillary detection and "interface" qubit) which is hyperfine-coupled to a spin-7/2 nucleus (the data storage qudit); this represents a Hilbert space extension of $d = 8$ over the qubit space.

We remark that a quantum information processor unit (based on the ^{123}Sb donor in Si) has already been realized experimentally that exhibits these properties and all of the necessary operations for implementation of the protocol [40]. We would expect our protocol to yield substantially enhanced relaxation and coherence times, thereby offering a highly efficient structure for robust quantum data storage.

A schematic diagram is presented in Fig. 1. The quantum state to be protected, $|\psi\rangle = \alpha|0\rangle + \beta e^{i\phi}|1\rangle$, will be encoded into $U_{\text{enc}}|\psi\rangle = |\Psi^{\text{enc}}\rangle = \alpha|0_L\rangle + \beta e^{i\phi}|1_L\rangle$ by the encoding pulse sequence in Fig. 1(c), with logical code words

$$|0_L\rangle = \sqrt{\frac{3}{10}}\left|-\frac{7}{2}\right\rangle + \sqrt{\frac{7}{10}}\left|+\frac{3}{2}\right\rangle \text{ and } |1_L\rangle = -\sqrt{\frac{7}{10}}\left|-\frac{3}{2}\right\rangle + \sqrt{\frac{3}{10}}\left|+\frac{7}{2}\right\rangle. \quad (1)$$

This logical qubit encoding is designed to handle phase (Z), shift (X), and phase-shift (Y) errors simultaneously (see Appendix A).

Under the assumption that the states of S_Z form good eigenstates (which is reasonable for a spin system in a significant magnetic field along z), we follow the procedure in Ref. [35] to find the time evolution of the density matrix in the presence of magnetic field fluctuations in all directions,

$$\rho(t) = \rho(0) + \sum_{k,i} E_{k,i}\rho(0)E_{k,i}^{\dagger}, \quad (2)$$

with error operators

$$E_{k,i} \sim \sqrt{\frac{(t/T_{\text{relax},i})^k}{k!}} S_i^k, \quad (3)$$

where $i = X$, Y, or Z; $k = 1, \ldots, \infty$; and t is short compared to $T_{\text{relax},i}$, the typical relaxation time of the system (see Appendix B).

TABLE I. Code words and error spaces for spin 7/2 encoding.

Logical code word	Representation in z basis
$\|0_L\rangle$	$\sqrt{+\frac{3}{10}}\|-\frac{7}{2}\rangle + \sqrt{\frac{7}{10}}\|+\frac{3}{2}\rangle$
$\|1_L\rangle$	$-\sqrt{\frac{7}{10}}\|-\frac{3}{2}\rangle + \sqrt{\frac{3}{10}}\|+\frac{7}{2}\rangle$
$S_X\|0_L\rangle$	$+\sqrt{\frac{1}{10}}\|-\frac{5}{2}\rangle + \sqrt{\frac{1}{2}}\|+\frac{1}{2}\rangle + \sqrt{\frac{2}{10}}\|+\frac{5}{2}\rangle$
$S_X\|1_L\rangle$	$-\sqrt{\frac{2}{10}}\|-\frac{5}{2}\rangle - \sqrt{\frac{1}{2}}\|-\frac{1}{2}\rangle + \sqrt{\frac{1}{10}}\|+\frac{5}{2}\rangle$
$iS_Y\|0_L\rangle$	$-\sqrt{\frac{1}{10}}\|-\frac{5}{2}\rangle + \sqrt{\frac{1}{2}}\|+\frac{1}{2}\rangle - \sqrt{\frac{2}{10}}\|+\frac{5}{2}\rangle$
$iS_Y\|1_L\rangle$	$-\sqrt{\frac{2}{10}}\|-\frac{5}{2}\rangle + \sqrt{\frac{1}{2}}\|-\frac{1}{2}\rangle + \sqrt{\frac{1}{10}}\|+\frac{5}{2}\rangle$
$S_Z\|0_L\rangle$	$-\sqrt{\frac{7}{10}}\|-\frac{7}{2}\rangle + \sqrt{\frac{3}{10}}\|+\frac{3}{2}\rangle$
$S_Z\|1_L\rangle$	$+\sqrt{\frac{3}{10}}\|-\frac{3}{2}\rangle + \sqrt{\frac{7}{10}}\|+\frac{7}{2}\rangle$

We may assume that for times short compared to T_{relax}, only first-order ($i = 1$) terms contribute significantly to the error, i.e.,

$$\rho(t) = (1-\epsilon)I + \epsilon_X S_X \rho(0) S_X^\dagger + \epsilon_Y S_Y \rho(0) S_Y^\dagger + \epsilon_Z S_Z \rho(0) S_Z^\dagger + O(\epsilon^2 \text{ and higher}), \tag{4}$$

where $\epsilon_i \sim t/T_{\text{relax},i}$ is indicative of the scale of the error. We note here that unlike for spin qubits (for which $S_i^2 = I$), the higher-order qudit spin operators S_i^k contribute to higher-order errors.

Thus, following application of the error operator, the state becomes corrupted to

$$\begin{aligned}|\Psi^{\text{enc+error}}\rangle = {} & \sqrt{1-\epsilon}(\alpha|0_L\rangle + \beta e^{i\phi}|1_L\rangle) \\ & + \sqrt{\epsilon_X}(\alpha S_X|0_L\rangle + \beta e^{i\phi} S_X|1_L\rangle) \\ & + \sqrt{\epsilon_Y}(\alpha S_Y|0_L\rangle + \beta e^{i\phi} S_Y|1_L\rangle) \\ & + \sqrt{\epsilon_Z}(\alpha S_Z|0_L\rangle + \beta e^{i\phi} S_Z|1_L\rangle) + \text{ higher order}.\end{aligned} \tag{5}$$

As required if we are to use these states for quantum error correction, the states in this superposition satisfy the Knill-Laflamme criteria [7]. Under the action of the error operator the original code words $|0_L\rangle$, $|1_L\rangle$ are transformed to span the states $|0_L\rangle$, $|1_L\rangle$, $S_X|0_L\rangle$, $S_X|1_L\rangle$, $S_Y|0_L\rangle$, $S_Y|1_L\rangle$, $S_Z|0_L\rangle$, and $S_Z|1_L\rangle$ (see Table I), and these eight states are mutually orthonormal; they satisfy the conditions

$$\begin{aligned}\langle 0_L|S_i^l S_j^k|1_L\rangle &= 0 \text{ and} \\ \langle 0_L|S_i^l S_j^k|0_L\rangle = \langle 1_L|S_i^l S_j^k|1_L\rangle &= \delta_{ij}\delta_{lk},\end{aligned} \tag{6}$$

where $i, j = X, Y$, or Z and $l, k = 0$ or 1.

This implies that first-order errors on the logical state can be detected and corrected. Indeed, the sequence of pulses in Fig. 1(d) transforms the corrupted state (see Appendix D) into

$$\begin{aligned}U_{\text{dec}}|\Psi^{\text{enc+error}}\rangle = {} & \sqrt{1-\epsilon}\left(\alpha\left|-\frac{7}{2}\right\rangle + \beta e^{i\phi}\left|+\frac{7}{2}\right\rangle\right) \\ & + \sqrt{\epsilon_Z}\left(\alpha\left|-\frac{5}{2}\right\rangle + \beta e^{i\phi}\left|+\frac{5}{2}\right\rangle\right) \\ & + \sqrt{\epsilon_X}\left(\alpha\left|-\frac{3}{2}\right\rangle + \beta e^{i\phi}\left|+\frac{3}{2}\right\rangle\right) \\ & + \sqrt{\epsilon_Y}\left(\alpha\left|-\frac{1}{2}\right\rangle + \beta e^{i\phi}\left|+\frac{1}{2}\right\rangle\right) \\ & + \text{ higher order}.\end{aligned} \tag{7}$$

Following this decoding, a conditional excitation and measurement of the ancillary electron spin reveals whether the state is corrupted, and if so, the nature of the error. For example, a conditional swap from the nuclear $|-1/2\rangle, |+1/2\rangle$ subspace onto the electron ancilla generates a full electron-nuclear state of the form

$$\begin{aligned}|\Psi\rangle \sim {} & (\text{remaining terms})|0_{\text{ancilla}}\rangle \\ & + \sqrt{\epsilon_Y}\left(\alpha\left|-\frac{1}{2}\right\rangle + \beta e^{i\phi}\left|+\frac{1}{2}\right\rangle\right)|1_{\text{ancilla}}\rangle.\end{aligned} \tag{8}$$

If a subsequent projective measurement of the electron spin ancilla yields $|1\rangle$, we conclude that there was a S_Y error. If it yields $|0\rangle$, we can iterate as shown in Fig. 1 until the ancilla measurement yields $|1\rangle$. In this way we can identify the error cases (i.e., which of I, S_Z, S_X, or S_Y occurred), the individual terms of Eq. (7), and thus the original state $|\psi\rangle$.

The algorithm fails if the measured state does not yield one of these four (I, S_Z, S_X, S_Y) outcomes; this corresponds to a higher-order error case and has probability of order $(t/T_{\text{relax}})^2$. Therefore, as long as t is short compared to T_{relax} we obtain a fidelity gain corresponding to the first-order error probability. This is shown in Fig 2, which shows how the fidelity varies with t/T_{relax} under the assumption that the relaxation rate is isotropic (i.e., rates for X, Y, or Z errors are equal) with (orange) and without (blue) error correction.

The operations implementing this protocol on an electronic $S = 1/2$ qubit coupled to a nuclear spin qudit $I = 7/2$ correspond to simple microwave or radio-frequency pulses, as long as the spin Hamiltonian includes a Zeeman term (provided by an external magnetic field), a hyperfine coupling between the electronic and nuclear spins, and a term (such as a nuclear quadrupole interaction) lifting the degeneracy of transitions within the nuclear manifold. In a realistic apparatus encoding and decoding pulse sequences have durations of the order of tens of microseconds [39,44–46]. For a condensed matter spin system with relaxation times of the order of tens of milliseconds (as has been reported in various isotopically enriched materials [47,48]), $t/T_{\text{relax}} \sim 10^3$, and our scheme extends the qubit coherence by multiple orders of magnitude.

Given that the entire encoding and decoding procedure requires about 40 pulses, the effectiveness of the protocol is naturally sensitive to the fidelity of the individual spin manipulation operations. Figure 2 shows how imperfect magnetic resonance pulses compromise the overall fidelity; individual pulse fidelities must exceed about 0.99 for the protocol to offer any advantage over natural relaxation.

In particular physical systems the range of available operations is wider, and this can be exploited to implement the protocol more efficiently with fewer operations. For example, through electric field induced modulation of the nuclear quadrupole interaction of ^{123}Sb nuclear spins in Si, it is possible to drive resonant $\Delta m = \pm 2$ transitions within the $I = 7/2$ nuclear spin manifold [40]; this significantly reduces the number of SWAP operations (π pulses) required in the encoding

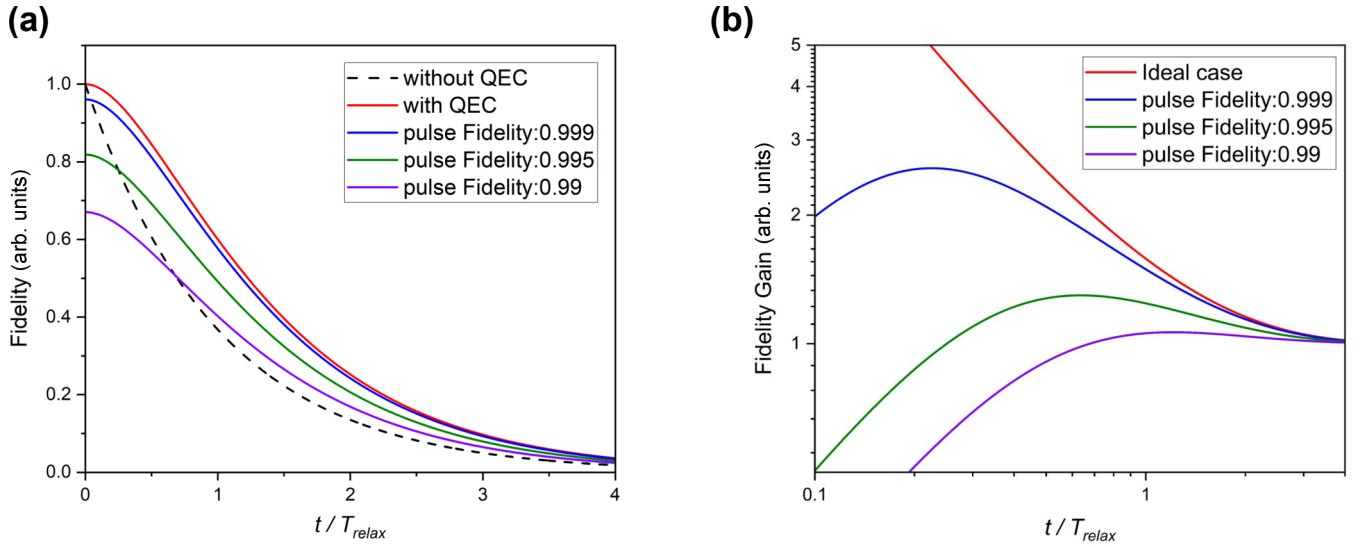

FIG. 2. (a) The qubit fidelity as a function of time without (black) and with (red) error correction. The detrimental effect of imperfect magnetic resonance pulses is simulated for pulse fidelities of 0.999 (blue), 0.995 (green), and 0.99 (purple). (b) Fidelity gain (defined as the ratio of the infidelities of the uncorrected and corrected cases) for a range of pulse fidelities.

and decoding sequences and therefore relaxes the threshold for the pulse fidelity to 0.98.

Interestingly, the effectiveness of our protocol corresponds to what is possible in distance-3 codes in qubit error correction. (Distance-3 codes fail when simultaneous errors occur on more than two qubits; for a single-qubit error rate $1/T_{\text{relax}}$, the probability of two or more simultaneous errors in time t is $\sim(t/T_{\text{relax}})^2$, as we find above for our protocol.) Based on the quantum Hamming bound [49], the minimal number of qubits for building a distance-3 error correction code is 5, requiring a Hilbert space dimension of 32. Thus, our spin-7/2 qudit-based code has advantages over the existing qubit counterpart, in both the size of Hilbert space and the number of actual physical objects over which quantum control is required. We can generalize this resource argument: for a qubit-based $[n, k, 2t+1]$ code, the quantum Hamming bound

$$2^k \sum_{l=0}^{t} 3^l \binom{n}{l} \leqslant 2^n \tag{9}$$

determines the number of qubits required [49]. Thus a distance-5 encoding of a single logical qubit requires 11 physical qubits, i.e., a Hilbert space of dimension 2048.

The strategy for fault-tolerant encoding on spin qudits can be generalized as follows. Inspired by previous studies and the basic concept of the original GKP code, we suggest code words comprising $\sim N$ periodic terms on a $\sim 4N^2$-dimensional qudit. The logical code words supporting Nth order error correction can be generated in the form

$$\begin{aligned} |0_L\rangle &= a_0|-S\rangle + \sum_{i=1}^{N} a_i|-S+(Ai-B)\rangle \\ |1_L\rangle &= b_0|+S\rangle + \sum_{i=1}^{N} b_i|+S-(Ai-B)\rangle, \end{aligned} \tag{10}$$

where the parameters S, A, B, a_i, b_i are chosen to satisfy the Knill-Laflamme criteria (see Appendices A and C). Here, we present example cases of solutions corresponding to $d = 4N(N+1)$ and $d = 4N(N+1)+2$, as shown in Table II.

The example code word in Table II shows that distance-5 encoding for a spin qudit is possible with a system of only $d = 24$. These codes can offer orders of magnitude improved resource efficiency compared to qubit-based encodings.

A previous Bosonic quantum error correction proposal exploiting an analogy with generalized Pauli matrix formalism was suggested in Ref. [10], but this sequence is somewhat different from the perspective of required resources. In the GKP code formalism and its expansion to harmonic oscillator systems, each sign of amplitude damping ($\pm X$) and phase damping ($\pm Z$) is mapped into a different basis [50]. Error correction up to Nth order requires a Hilbert space dimension of $2 \times (2N+1) \times (2N+1)$, resulting in minimum $d = 18$ basis states for first-order correction, and $d = 50$ for up to second-order correction, about twice the resource compared to our proposal here.

We also note that a Hilbert space comprising multiple qudits can also provide a viable code space (for example, encoding for second-order error correction using four spin-7/2 qudits; see Appendix C 1), and can offer optimized code words when the size or number of spins are limited in specific experimental implementations.

Finally, we address the comparison between T_1 (bit error) and T_2 (phase error) relaxation in spin systems. Often in the solid state T_2 is found to be much shorter than T_1; practical proposals have therefore concentrated on phase error protection [35] for pragmatic reasons. However, it has been found in certain systems that careful optimization of the environment can significantly reduce phase relaxation, for example, by isotopically purifying the ^{28}Si or ^{12}C host environments for P donors [48,51] or NV centers [47], respectively, or by engineering the ligand environment in molecular magnets [52]. When phase relaxation mechanisms are suppressed, T_1

TABLE II. Example code words for Nth-order error correction on high-spin qudits.

Nth order, d-dim	$\|0_L\rangle$ Representation in z basis	$\|1_L\rangle$ Representation in z basis
$N=1, d=8$ (spin 7/2)	$+\sqrt{\frac{3}{10}}\|-\frac{7}{2}\rangle+\sqrt{\frac{7}{10}}\|+\frac{3}{2}\rangle$	$-\sqrt{\frac{3}{10}}\|+\frac{7}{2}\rangle+\sqrt{\frac{7}{10}}\|-\frac{3}{2}\rangle$
$N=1, d=10$ (spin 9/2)	$+\sqrt{\frac{1}{4}}\|-\frac{9}{2}\rangle+\sqrt{\frac{3}{4}}\|+\frac{3}{2}\rangle$	$+\sqrt{\frac{1}{4}}\|+\frac{9}{2}\rangle+\sqrt{\frac{3}{4}}\|-\frac{3}{2}\rangle$
$N=2, d=24$ (spin 23/2)	$+\sqrt{\frac{125}{1482}}\|-\frac{23}{2}\rangle+\sqrt{\frac{874}{1482}}\|-\frac{5}{2}\rangle+\sqrt{\frac{483}{1482}}\|+\frac{15}{2}\rangle$	$-\sqrt{\frac{125}{1482}}\|+\frac{23}{2}\rangle+\sqrt{\frac{874}{1482}}\|+\frac{5}{2}\rangle+\sqrt{\frac{483}{1482}}\|-\frac{15}{2}\rangle$
$N=2, d=26$ (spin 25/2)	$+\sqrt{\frac{1}{16}}\|-\frac{25}{2}\rangle+\sqrt{\frac{10}{16}}\|-\frac{5}{2}\rangle+\sqrt{\frac{5}{16}}\|+\frac{15}{2}\rangle$	$+\sqrt{\frac{1}{16}}\|+\frac{25}{2}\rangle+\sqrt{\frac{10}{16}}\|+\frac{5}{2}\rangle+\sqrt{\frac{5}{16}}\|-\frac{15}{2}\rangle$
$N=3, d=50$ (spin 49/2)	$+\sqrt{\frac{1}{64}}\|-\frac{49}{2}\rangle+\sqrt{\frac{21}{64}}\|-\frac{21}{2}\rangle+\sqrt{\frac{35}{64}}\|+\frac{7}{2}\rangle+\sqrt{\frac{7}{64}}\|+\frac{35}{2}\rangle$	$+\sqrt{\frac{1}{64}}\|+\frac{49}{2}\rangle+\sqrt{\frac{21}{64}}\|+\frac{21}{2}\rangle+\sqrt{\frac{35}{64}}\|-\frac{7}{2}\rangle+\sqrt{\frac{7}{64}}\|-\frac{35}{2}\rangle$

relaxation will become increasingly important, and error correction algorithms addressing both error classes become important. Furthermore, the strategy that we present here allows for the possibility of checking for each error independently. Under the circumstances that $T_2 << T_1$ and projective measurement of the ancilla electron spin is expensive, an optimal practical implementation might check more frequently for S_Z errors than for S_X and S_Y errors.

ACKNOWLEDGMENTS

This project was supported by the European Union's Horizon 2020 research and innovation program under Grants No. 862893 (FATMOLS) and No. 863098 (SPRING). J.L. is supported by the Royal Society through a University Research Fellowship.

APPENDIX A: CANDIDATES FOR LOGICAL QUBIT $|0_L\rangle$ AND $|1_L\rangle$ STATES

1. Encoding for first-order error correction

In order to enable first-order error correction for S_X, S_Y, and S_Z, the logical qubits, $|0_L\rangle$ and $|1_L\rangle$, should satisfy the Knill-Laflamme criteria

$$\langle 0_L|S_i^l S_j^k|1_L\rangle = 0,$$
$$\langle 0_L|S_i^l S_j^k|0_L\rangle = \langle 1_L|S_i^l S_j^k|1_L\rangle = \delta_{i,j}\delta_{l,k}, \tag{A1}$$

where $i, j = X, Y$, or Z and $l, k = 0$ or 1. It is not strictly necessary for the second equation to be identical to the Kronecker delta. However, it (a) helps to distinguish the corrupted state from pure states and (b) does not change the minimum hardware required for the QEC. (While it is not necessary for all error states to be orthogonal to each other, they need to be linearly independent to ensure that different errors can be distinguished. Hence, lifting the orthogonality condition implied by the Kronecker delta would not change the dimension of the vector space spanned by the logic qubits and all possible error states.) Effectively, Eq. (A1) requires the following eight states,

$$|0_L\rangle, S_X|0_L\rangle, S_Y|0_L\rangle, S_Z|0_L\rangle, |1_L\rangle, S_X|1_L\rangle, S_y|1_L\rangle, S_z|1_L\rangle \tag{A2}$$

to be nonzero and mutually orthogonal. The smallest Hilbert space that can accommodate these states is eight-dimensional, in which case the eight states in Eq. (A2) form a complete orthogonal basis set. Hence, the minimum spin qudit that can potentially allow corrections for all first-order errors is a $S = 7/2$ system.

Finding all possible solutions for Eq. (A1) with $S = 7/2$ is cumbersome as it involves solving multiple coupled second-order polynomials. Thus, we confirmed the existence of $|0_L\rangle$ and $|1_L\rangle$ combinations by finding examples satisfying Eq. (A1) numerically. The simplest solution we found is

$$|0_L\rangle = \sqrt{\frac{3}{10}}\left|-\frac{7}{2}\right\rangle + \sqrt{\frac{7}{10}}\left|+\frac{3}{2}\right\rangle$$
$$|1_L\rangle = -\sqrt{\frac{7}{10}}\left|-\frac{3}{2}\right\rangle + \sqrt{\frac{3}{10}}\left|+\frac{7}{2}\right\rangle. \tag{A3}$$

It is straightforward to verify that these logical qubits meet the criteria listed in Eq. (A1). It is worth pointing out, however, that this solution (which was previously identified by Gross [38]) is not unique. For example, the following states,

$$|0_L\rangle = -\sqrt{\frac{21}{64}}\left|-\frac{5}{2}\right\rangle + \sqrt{\frac{21}{64}}\left|-\frac{1}{2}\right\rangle + \sqrt{\frac{7}{64}}\left|+\frac{3}{2}\right\rangle + \sqrt{\frac{15}{64}}\left|+\frac{7}{2}\right\rangle$$
$$|1_L\rangle = -\sqrt{\frac{15}{64}}\left|-\frac{7}{2}\right\rangle - \sqrt{\frac{7}{64}}\left|-\frac{3}{2}\right\rangle - \sqrt{\frac{21}{64}}\left|+\frac{1}{2}\right\rangle + \sqrt{\frac{21}{64}}\left|+\frac{5}{2}\right\rangle, \tag{A4}$$

can also be used for correcting all first-order errors. However, the encoding and decoding pulse sequences for Eq. (A4), when implemented on a spin qudit, are significantly more complicated than those for Eq. (A3); thus, we choose to use Eq. (A3) as the working example for all discussions presented in this work.

For qudits with $S > 7/2$, similar code words for first-order QEC can be found easily. For instance, in $S = 9/2$ systems (e.g., the nuclear spins of Bi and Sr) the simplest logical qubits are

$$|0_L\rangle = -\sqrt{\frac{1}{4}}\left|-\frac{9}{2}\right\rangle + \sqrt{\frac{3}{4}}\left|+\frac{3}{2}\right\rangle$$
$$|1_L\rangle = +\sqrt{\frac{3}{4}}\left|-\frac{3}{2}\right\rangle + \sqrt{\frac{1}{4}}\left|+\frac{9}{2}\right\rangle. \tag{A5}$$

APPENDIX B: TIME EVOLUTION OF THE DENSITY MATRIX

We follow closely the treatment established by Chiesa *et al.* in the Supporting Information of Ref. [35]. We extend their treatment to consider the effect on the qudit of magnetic

field fluctuations in all directions by describing the qudit-environment interaction via couplings of the form $S_i \otimes \boldsymbol{B}$, where $S_i = S_X, S_Y, S_Z$ and $\boldsymbol{B}$ is a suitable operator acting on bath. Based on the standard derivation of the Lindblad master equation, the time evolution of the density matrix is

$$\begin{aligned}\frac{d\rho(t)}{dt} &= \gamma_X\left(S_X\rho(t)S_X^\dagger - \frac{1}{2}\{S_X^2, \rho(t)\}\right)\\ &+ \gamma_Y\left(S_Y\rho(t)S_Y^\dagger - \frac{1}{2}\{S_Y^2, \rho(t)\}\right)\\ &+ \gamma_Z\left(S_Z\rho(t)S_Z^\dagger - \frac{1}{2}\{S_Z^2, \rho(t)\}\right),\end{aligned} \tag{B1}$$

where $\gamma_i = \frac{2}{T_{\text{relax},i}}$. Following the procedure of Chiesa *et al.* yields the time evolution of the density matrix

$$\begin{aligned}\rho(t) = \rho(0) + \sum_{i=X,Y,Z}\sum_{k=1}^{\infty} e^{-\frac{(\gamma_X S_X^2+\gamma_Y S_Y^2+\gamma_Z S_Z^2)}{2}t}\frac{(\gamma_i t)^k}{k!}S_i^k\rho(0)S_i^{\dagger k}\\ \times\ e^{-\frac{(\gamma_X S_X^2+\gamma_Y S_Y^2+\gamma_Z S_Z^2)}{2}t}.\end{aligned} \tag{B2}$$

Thus, the Kraus error operators can be written as

$$E_{k,i} = \sqrt{\frac{(\gamma_i t)^k}{k!}}e^{-\frac{(\gamma_X S_X^2+\gamma_Y S_Y^2+\gamma_Z S_Z^2)}{2}t}S_i^k \approx \sqrt{\frac{(\gamma_i t)^k}{k!}}S_i^k \tag{B3}$$

in the short-time limit, yielding the form given in Eq. (3) of the main manuscript.

APPENDIX C: ENCODING FOR SECOND- AND HIGHER-ORDER ERROR CORRECTION

One can apply the same strategy to develop an efficient protocol for correcting high-order quantum errors using qudits. To correct an Nth-order error, the logical qubits should meet the following criteria:

$$\langle 0_L|S_i^l S_j^k|1_L\rangle = 0, \quad \langle 0_L|S_i^l S_j^k|0_L\rangle = \langle 1_L|S_i^l S_j^k|1_L\rangle, \tag{C1}$$

where $i, j = X, Y$, or Z and $l, k = 0, 1 \ldots N$.

Here, we propose a general approach for designing the logical qubits within $4N(N+1)$- or $4N(N+1)+2$-dimensional spaces, hence enabling any Nth-order error correction to be implemented with a $S = [4N(N+1)-1]/2$ or a $S = [4N(N+1)+1]/2$ qudit, respectively.

In the case of $S = [4N(N+1)+1]/2$, both $|0_L\rangle$ and $|1_L\rangle$ are superpositions of the $N+1$ S_z eigenstates such that

$$\begin{aligned}|0_L\rangle &= a_0|-S\rangle + \sum_{i=1}^{N} a_i|-S+(Ai-B)\rangle\\ |1_L\rangle &= b_0|+S\rangle + \sum_{i=1}^{N} b_i|+S-(Ai-B)\rangle,\end{aligned} \tag{C2}$$

where $A = 4N+2$, $B = 0$, and the coefficients for $|0_L\rangle$, $\{a_i\}$ $(i = 0, 1 \ldots N)$, are calculated by solving the following equations:

$$\langle 0_L|0_L\rangle = 1, \quad \langle 0_L|S_X^j S_Z S_X^j|0_L\rangle = 0, \tag{C3}$$

where $0 \leqslant j \leqslant N-1$. Equation (C3) imposes $N+1$ constraints on $\{a_i\}$. Indeed, Eq. (C3) can be rewritten as $N+1$ real linear equations with $\{|a_i|^2\}$ being $N+1$ independent variables. Solving them gives a set of positive $|a_i|^2$ and we choose the root $a_i = |a_i|$ for constructing $|0_L\rangle$. $|1_L\rangle$ can then be defined with $b_0 = a_0$ and $b_i = a_i$ for $1 \leqslant i \leqslant N$.

In the case of $S = [4N(N+1)-1]/2$, both $|0_L\rangle$ and $|1_L\rangle$ are constructed in similar form, but with $A = 4N+2$ and $B = 1$. The coefficients are obtained with almost the same conditions, except for b_0, which is defined by $b_0 = -a_0$.

We do not offer a proof that this approach works in all cases, though we find that it works for a wide range of cases that we have explored, and we have found none where it does not.

By way of illustration, the approach yields logical qubits for third-order QEC ($N = 3$) on a $S = 47/2$ system, given by

$$\begin{aligned}|0_L\rangle &= +\sqrt{\frac{16807}{796302}}\left|-\frac{47}{2}\right\rangle + \sqrt{\frac{260145}{796302}}\left|-\frac{21}{2}\right\rangle + \sqrt{\frac{425867}{796302}}\left|+\frac{7}{2}\right\rangle + \sqrt{\frac{93483}{796302}}\left|+\frac{35}{2}\right\rangle\\ |1_L\rangle &= -\sqrt{\frac{16807}{796302}}\left|+\frac{47}{2}\right\rangle + \sqrt{\frac{260145}{796302}}\left|+\frac{21}{2}\right\rangle + \sqrt{\frac{425867}{796302}}\left|-\frac{7}{2}\right\rangle + \sqrt{\frac{93483}{796302}}\left|-\frac{35}{2}\right\rangle,\end{aligned} \tag{C4}$$

and fourth-order QEC ($N = 4$) on a $S = 81/2$ system, given by

$$\begin{aligned}|0_L\rangle &= +\sqrt{\frac{1}{256}}\left|-\frac{81}{2}\right\rangle + \sqrt{\frac{36}{256}}\left|-\frac{45}{2}\right\rangle + \sqrt{\frac{126}{256}}\left|-\frac{9}{2}\right\rangle + \sqrt{\frac{84}{256}}\left|+\frac{27}{2}\right\rangle + \sqrt{\frac{9}{256}}\left|+\frac{63}{2}\right\rangle\\ |1_L\rangle &= +\sqrt{\frac{1}{256}}\left|+\frac{81}{2}\right\rangle + \sqrt{\frac{36}{256}}\left|+\frac{45}{2}\right\rangle + \sqrt{\frac{126}{256}}\left|+\frac{9}{2}\right\rangle + \sqrt{\frac{84}{256}}\left|-\frac{27}{2}\right\rangle + \sqrt{\frac{9}{256}}\left|-\frac{63}{2}\right\rangle,\end{aligned} \tag{C5}$$

which satisfy all KL criteria in Eq. (C1).

Finally, the spin operator identities $\sum_{i=X,Y,Z} S_i^2 = S(S+1)$ and $[S_i, S_j] = \mathrm{i}S_k$ encapsulate the behavior of the physical system that embodies the quantum information and is subject to noise. We note that they constrain the evolution of second-order errors in such a way that it may be possible to perform high-order QEC ($N \geqslant 2$) with a qudit smaller than $S = [4N(N+1) - 1]/2$.

1. Encoding for multiple qudits

The same approach may be used to build logical qubits for a physical system comprising multiple qudits. For example, for the three spin-3/2 qudits, (labeled A, B, and C) the code words given by

$$\begin{aligned} |0_L\rangle &= +\sqrt{\frac{1}{4}}\left|-\frac{3}{2}\right\rangle_{A,B,C} + \sqrt{\frac{3}{4}}\left|+\frac{1}{2}\right\rangle_{A,B,C} \\ |1_L\rangle &= +\sqrt{\frac{1}{4}}\left|+\frac{3}{2}\right\rangle_{A,B,C} + \sqrt{\frac{3}{4}}\left|-\frac{1}{2}\right\rangle_{A,B,C} \end{aligned} \tag{C6}$$

satisfy all KL criteria in Eq. (C1) up to first order. (Here, the notation $|m_I\rangle_{A,B,C}$ represents the tensor product of three spin states, $|m_I\rangle_A \otimes |m_I\rangle_B \otimes |m_I\rangle_C$.) And for four spin-7/2 qudits, (labeled A, B, C, and D), the code words given by

$$\begin{aligned} |0_L\rangle &= +\sqrt{\frac{2}{16}}\left|-\frac{7}{2}\right\rangle_{A,B,C,D} + \sqrt{\frac{7}{16}}\left|-\frac{3}{2}\right\rangle_{A,B,C,D} + \sqrt{\frac{7}{16}}\left|+\frac{5}{2}\right\rangle_{A,B,C,D} \\ |1_L\rangle &= +\sqrt{\frac{2}{16}}\left|+\frac{7}{2}\right\rangle_{A,B,C,D} + \sqrt{\frac{7}{16}}\left|+\frac{3}{2}\right\rangle_{A,B,C,D} - \sqrt{\frac{7}{16}}\left|-\frac{5}{2}\right\rangle_{A,B,C,D}, \end{aligned} \tag{C7}$$

satisfy all KL criteria in Eq. (C1) up to second order.

APPENDIX D: PULSE SEQUENCES FOR ENCODING AND DECODING LOGICAL QUBITS

Here, we discuss the physical operations that implement the spin-7/2 first-order protection presented in the main manuscript and in Appendix A 1.

1. Encoding pulse sequence

Without loss of generality, we may assume a qubit $|\psi\rangle$ is initially stored in a superposition between $|-7/2\rangle$ and $|-5/2\rangle$ states, such that $|\psi\rangle = \alpha|-7/2\rangle + \beta e^{\mathrm{i}\theta}|-5/2\rangle$, where α, β, and θ encode the quantum information. In the S_Z basis,

$$|\psi\rangle = [\alpha, \quad \beta e^{\mathrm{i}\theta}, \quad 0, \quad 0, \quad 0, \quad 0, \quad 0, \quad 0]^T. \tag{D1}$$

The first four pulses in the encoding sequence [Fig. 1(c) in the main text], i.e., the first π pulse, $U_{\theta 1}$, $U_{\theta 2}$, and the second π pulse, transform $|\psi\rangle$ into

$$\left[\sqrt{\frac{3}{10}}\alpha, \quad -\sqrt{\frac{7}{10}}\beta e^{i\theta}, \quad \sqrt{\frac{7}{10}}\alpha, \quad \sqrt{\frac{3}{10}}\beta e^{i\theta}, \quad 0, \quad 0, \quad 0, \quad 0\right]^T. \tag{D2}$$

The subsequent eight π pulses further transform the state into the encoded state

$$|\Psi^{\mathrm{enc}}\rangle = \left[\sqrt{\frac{3}{10}}\alpha, \quad 0, \quad -\sqrt{\frac{7}{10}}\beta e^{i\theta}, \quad 0, \quad 0, \quad \sqrt{\frac{7}{10}}\alpha, \quad 0, \quad \sqrt{\frac{3}{10}}\beta e^{i\theta}\right]^T = \alpha|0_L\rangle + \beta e^{i\theta}|1_L\rangle. \tag{D3}$$

As shown in Eq. (D3), the entire encoding sequence maps the original qubit onto the corresponding superposition of QEC logical qubit states $|0_L\rangle$ and $|1_L\rangle$.

2. Decoding pulse sequence

After the storage period during which first-order errors may occur, the density matrix of the nuclear spin can be written as

$$\rho(t) = (1-\epsilon)I + \epsilon_X S_X \rho(0) S_X^\dagger + \epsilon_Y S_Y \rho(0) S_Y^\dagger + \epsilon_Z S_Z \rho(0) S_Z^\dagger + O(\epsilon^2), \tag{D4}$$

where $\epsilon_i \sim t/T_{\mathrm{relax},i}$ is indicative of the scale of the error. Interpreting the decoding sequence using the general form of Eq. (D4) can be laborious. However, as we discussed in the previous section, the logical qubit states and their first-order errors form an orthogonal basis for the Hilbert state [Eq. (A2)]. Therefore, we demonstrate the decoding sequence for the states $|\Psi^{\mathrm{enc}}\rangle$, $S_X|\Psi^{\mathrm{enc}}\rangle$, $S_X|\Psi^{\mathrm{enc}}\rangle$, and $S_Y|\Psi^{\mathrm{enc}}\rangle$ individually. As we will show in the following section, the decoding sequence converts the states in Eq. (A2) into another set of orthogonal states that are spectroscopically distinguishable, allowing errors to be identified using the corresponding projective measurements. The general error form is the linear combination of these decoupled orthogonal states.

a. Error free

If no error occurs, the spin remains in the $|\Psi^{\text{enc}}\rangle$ state. To decode this state, the first seven successive π pulses in the decoding sequence U_{dec} transform $|\Psi^{\text{enc}}\rangle$ into

$$\left[\sqrt{\frac{3}{10}}\alpha, \quad \sqrt{\frac{7}{10}}\alpha, \quad 0, \quad 0, \quad 0, \quad 0, \quad -\sqrt{\frac{7}{10}}\beta e^{i\theta}, \quad \sqrt{\frac{3}{10}}\beta e^{i\theta}\right]^T, \tag{D5}$$

and the subsequent two simultaneous $U_{-\theta 1}$ pulses further rotate it to the state

$$\left[\alpha, \quad 0, \quad 0, \quad 0, \quad 0, \quad 0, \quad 0, \quad \beta e^{i\theta}\right]^T. \tag{D6}$$

The remaining pulses do not act on either $|-7/2\rangle$ or $|7/2\rangle$, so this is the final decoded state.

b. S_Z error

A S_Z error will lead to a nonzero component for the state

$$S_Z|\Psi^{\text{enc}}\rangle = \left[-\sqrt{\frac{7}{10}}\alpha, \quad 0, \quad \sqrt{\frac{3}{10}}\beta e^{i\theta}, \quad 0, \quad 0, \quad \sqrt{\frac{3}{10}}\alpha, \quad 0, \quad \sqrt{\frac{7}{10}}\beta e^{i\theta}\right]^T. \tag{D7}$$

To decode this component, the first seven π pulses in U_{dec} transform the state to

$$\left[-\sqrt{\frac{7}{10}}\alpha, \quad \sqrt{\frac{3}{10}}\alpha, \quad 0, \quad 0, \quad 0, \quad 0, \quad \sqrt{\frac{3}{10}}\beta e^{i\theta}, \quad \sqrt{\frac{7}{10}}\beta e^{i\theta}\right]^T, \tag{D8}$$

and the following two $U_{-\theta 1}$ pulses transform it to

$$[0, \quad \alpha, \quad 0, \quad 0, \quad 0, \quad 0, \quad \beta e^{i\theta}, \quad 0]^T, \tag{D9}$$

at which point the decoding process is complete. Any S_Z error is readily detectable by a subsequent projective measurement on the $m_I = \pm 5/2$ hyperfine transition of the electron spin ancilla.

c. S_X error

A S_X error will lead to a nonzero component for the state

$$S_X|\Psi^{\text{enc}}\rangle = \left[0, \quad +\sqrt{\frac{1}{10}}\alpha - \sqrt{\frac{4}{10}}\beta e^{i\theta}, \quad 0, \quad -\sqrt{\frac{5}{10}}\beta e^{i\theta}, \quad \sqrt{\frac{5}{10}}\alpha, \quad 0, \quad \sqrt{\frac{4}{10}}\alpha + \sqrt{\frac{1}{10}}\beta e^{i\theta}, \quad 0\right]^T. \tag{D10}$$

To decode this component, the first seven π pulses in U_{dec} transform the state to

$$\left[0, \quad 0, \quad +\sqrt{\frac{1}{10}}\alpha - \sqrt{\frac{4}{10}}\beta e^{i\theta}, \quad +\sqrt{\frac{5}{10}}\beta e^{i\theta}, \quad -\sqrt{\frac{5}{10}}\alpha, \quad \sqrt{\frac{4}{10}}\alpha + \sqrt{\frac{1}{10}}\beta e^{i\theta}, \quad 0, \quad 0\right]^T. \tag{D11}$$

The two following $U_{-\theta 1}$ pulses do not alter the state since they only act on the $\{|-7/2\rangle, |-5/2\rangle, |5/2\rangle$, and $|7/2\rangle\}$ subspace. Instead, the two π pulses and $U_{-\theta 3}$ subsequently transform the state to

$$\left[0, \quad 0, \quad -\sqrt{\frac{5}{10}}\beta e^{i\theta}, \quad +\sqrt{\frac{5}{10}}\alpha, \quad \sqrt{\frac{5}{10}}\beta e^{i\theta}, \quad -\sqrt{\frac{5}{10}}\alpha \quad 0, \quad 0\right]^T, \tag{D12}$$

which is further transformed by the subsequent five π pulses into

$$\left[0, \quad 0, \quad \sqrt{\frac{5}{10}}\alpha, \quad -\sqrt{\frac{5}{10}}\alpha, \quad -\sqrt{\frac{5}{10}}\beta e^{i\theta}, \quad -\sqrt{\frac{5}{10}}\beta e^{i\theta}, \quad 0, \quad 0\right]^T. \tag{D13}$$

The final part of the decoding sequence, consisting of two $U_{\theta 4}$ pulses and two π pulses, transforms the state into the form

$$[0, \quad 0, \quad \alpha, \quad 0, \quad 0, \quad \beta e^{i\theta}, \quad 0, \quad 0]^T, \tag{D14}$$

which allows any S_X error to be detected via a measurement on the $m_I = \pm 3/2$ hyperfine transition of the electron ancilla.

d. S_Y error

The underlying principle for decoding S_Y error is equivalent to that for S_X error, albeit the exact states involved are slightly different. A S_Y error will lead to the state

$$S_Y|\Psi^{\text{enc}}\rangle = \left[0, \quad -\sqrt{\frac{1}{10}}\alpha - \sqrt{\frac{4}{10}}\beta e^{i\theta}, \quad 0, \quad \sqrt{\frac{5}{10}}\beta e^{i\theta}, \quad \sqrt{\frac{5}{10}}\alpha, \quad 0, \quad -\sqrt{\frac{4}{10}}\alpha + \sqrt{\frac{1}{10}}\beta e^{i\theta}, \quad 0\right]^T. \tag{D15}$$

The first seven π pulses in U_{dec} transform the state to

$$\left[0, \quad 0, \quad -\sqrt{\frac{1}{10}}\alpha - \sqrt{\frac{4}{10}}\beta e^{i\theta}, \quad -\sqrt{\frac{5}{10}}\beta e^{i\theta}, \quad -\sqrt{\frac{5}{10}}\alpha, \quad \sqrt{\frac{4}{10}}\alpha - \sqrt{\frac{1}{10}}\beta e^{i\theta}, \quad 0, \quad 0\right]^T. \tag{D16}$$

The following two $U_{-\theta 1}$ pulses, the two π pulses, and $U_{-\theta 3}$ transform it to

$$\left[0, \quad 0, \quad +\sqrt{\frac{5}{10}}\beta e^{i\theta}, \quad -\sqrt{\frac{5}{10}}\alpha, \quad +\sqrt{\frac{5}{10}}\beta e^{i\theta}, \quad -\sqrt{\frac{5}{10}}\alpha \quad 0, \quad 0\right]^T. \tag{D17}$$

Then, the five π pulses reorder the state to

$$\left[0, \quad 0, \quad +\sqrt{\frac{5}{10}}\alpha, \quad +\sqrt{\frac{5}{10}}\alpha, \quad -\sqrt{\frac{5}{10}}\beta e^{i\theta}, \quad +\sqrt{\frac{5}{10}}\beta e^{i\theta}, \quad 0, \quad 0\right]^T. \tag{D18}$$

The final step for decoding is performed by the two $U_{\theta 4}$ pulses and two π pulses, resulting in the final state of

$$\left[0, \quad 0, \quad 0, \quad \alpha, \quad \beta e^{i\theta}, \quad 0, \quad 0, \quad 0\right]^T. \tag{D19}$$

Again, this state allows the detection of S_Y errors using projective measurements on the $m_I = \pm 1/2$ hyperfine transition of the electron spin ancilla.

[1] J. Preskill, Quantum computing in the NISQ era and beyond, Quantum **2**, 79 (2018).

[2] F. Arute, K. Arya, R. Babbush, D. Bacon, J. C. Bardin, R. Barends, R. Biswas, S. Boixo, F. G. S. L. Brandao, D. A. Buell, B. Burkett, Y. Chen, Z. Chen, B. Chiaro, R. Collins *et al.*, Quantum supremacy using a programmable superconducting processor, Nature (London) **574**, 505 (2019).

[3] Y. Wu, W.-S. Bao, S. Cao, F. Chen, M.-C. Chen, X. Chen, T.-H. Chung, H. Deng, Y. Du, D. Fan, M. Gong, C. Guo, C. Guo, S. Guo, L. Han *et al.*, Strong quantum computational advantage using a superconducting quantum processor, Phys. Rev. Lett. **127**, 180501 (2021).

[4] B. M. Terhal, Quantum error correction for quantum memories, Rev. Mod. Phys. **87**, 307 (2015).

[5] D. P. DiVincenzo and P. W. Shor, Fault-tolerant error correction with efficient quantum codes, Phys. Rev. Lett. **77**, 3260 (1996).

[6] R. Laflamme, C. Miquel, J. P. Paz, and W. H. Zurek, Perfect quantum error correcting code, Phys. Rev. Lett. **77**, 198 (1996).

[7] E. Knill and R. Laflamme, Theory of quantum error-correcting codes, Phys. Rev. A **55**, 900 (1997).

[8] E. Knill, R. Laflamme, and L. Viola, Theory of quantum error correction for general noise, Phys. Rev. Lett. **84**, 2525 (2000).

[9] R. Acharya, I. Aleiner, R. Allen, T. I. Andersen, M. Ansmann, F. Arute, K. Arya, A. Asfaw, J. Atalaya, R. Babbush, D. Bacon, J. C. Bardin, J. Basso, A. Bengtsson, S. Boixo *et al.*, Suppressing quantum errors by scaling a surface code logical qubit, Nature (London) **614**, 676 (2023).

[10] D. E. Gottesman, Stabilizer codes and quantum error correction, Ph.D. thesis, California Institute of Technology, 1997, doi:10.7907/rzr7-dt72.

[11] D. Gottesman, A. Kitaev, and J. Preskill, Encoding a qubit in an oscillator, Phys. Rev. A **64**, 012310 (2001).

[12] S. Pirandola, S. Mancini, S. L. Braunstein, and D. Vitali, Minimal qudit code for a qubit in the phase-damping channel, Phys. Rev. A **77**, 032309 (2008).

[13] K. Noh, S. M. Girvin, and L. Jiang, Encoding an oscillator into many oscillators, Phys. Rev. Lett. **125**, 080503 (2020).

[14] L. Hu, Y. Ma, W. Cai, X. Mu, Y. Xu, W. Wang, Y. Wu, H. Wang, Y. P. Song, C.-L. Zou, S. M. Girvin, L.-M. Duan, and L. Sun, Quantum error correction and universal gate set operation on a binomial bosonic logical qubit, Nat. Phys. **15**, 503 (2019).

[15] C. Flühmann and J. P. Home, Direct characteristic-function tomography of quantum states of the trapped-ion motional oscillator, Phys. Rev. Lett. **125**, 043602 (2020).

[16] N. Ofek, A. Petrenko, R. Heeres, P. Reinhold, Z. Leghtas, B. Vlastakis, Y. Liu, L. Frunzio, S. M. Girvin, L. Jiang, M. Mirrahimi, M. H. Devoret, and R. J. Schoelkopf, Extending the lifetime of a quantum bit with error correction in superconducting circuits, Nature (London) **536**, 441 (2016).

[17] P. Campagne-Ibarcq, A. Eickbusch, S. Touzard, E. Zalys-Geller, N. E. Frattini, V. V. Sivak, P. Reinhold, S. Puri, S. Shankar, R. J. Schoelkopf, L. Frunzio, M. Mirrahimi, and M. H. Devoret, Quantum error correction of a qubit encoded in grid states of an oscillator, Nature (London) **584**, 368 (2020).

[18] V. V. Albert, J. P. Covey, and J. Preskill, Robust encoding of a qubit in a molecule, Phys. Rev. X **10**, 031050 (2020).

[19] B. Royer, S. Singh, and S. M. Girvin, Stabilization of finite-energy Gottesman-Kitaev-Preskill states, Phys. Rev. Lett. **125**, 260509 (2020).
[20] L. M. Vandersypen, M. Steffen, G. Breyta, C. S. Yannoni, M. H. Sherwood, and I. L. Chuang, Experimental realization of Shor's quantum factoring algorithm using nuclear magnetic resonance, Nature (London) **414**, 883 (2001).
[21] N. A. Gershenfeld and I. L. Chuang, Bulk spin-resonance quantum computation, Science **275**, 350 (1997).
[22] D. G. Cory, A. F. Fahmy, and T. F. Havel, Ensemble quantum computing by NMR spectroscopy, Proc. Natl. Acad. Sci. **94**, 1634 (1997).
[23] J. A. Jones and M. Mosca, Implementation of a quantum algorithm on a nuclear magnetic resonance quantum computer, J. Chem. Phys. **109**, 1648 (1998).
[24] W. S. Warren, The usefulness of NMR quantum computing, Science **277**, 1688 (1997).
[25] M. N. Leuenberger and D. Loss, Quantum computing in molecular magnets, Nature (London) **410**, 789 (2001).
[26] J. Tejada, E. Chudnovsky, E. Del Barco, J. Hernandez, and T. Spiller, Magnetic qubits as hardware for quantum computers, Nanotechnology **12**, 181 (2001).
[27] A. Gaita-Ariño, F. Luis, S. Hill, and E. Coronado, Molecular spins for quantum computation, Nat. Chem. **11**, 301 (2019).
[28] M. Wasielewski, M. D. E. Forbes, N. L. Frank, K. Kowalski, G. D. Scholes, J. Yuen-Zhou, M. A. Baldo, D. E. Freedman, R. H. Goldsmith, T. Goodson III, M. L. Kirk, J. K. McCusker, J. P. Ogilvie, D. A. Shultz, S. Stoll, and K. B. Whaley, Exploiting chemistry and molecular systems for quantum information science, Nat. Rev. Chem. **4**, 490 (2020).
[29] A. Ardavan, O. Rival, J. J. L. Morton, S. J. Blundell, A. M. Tyryshkin, G. A. Timco, and R. E. P. Winpenny, Will spin-relaxation times in molecular magnets permit quantum information processing? Phys. Rev. Lett. **98**, 057201 (2007).
[30] R. Vincent, S. Klyatskaya, M. Ruben, W. Wernsdorfer, and F. Balestro, Electronic read-out of a single nuclear spin using a molecular spin transistor, Nature (London) **488**, 357 (2012).
[31] S. Thiele, F. Balestro, R. Ballou, S. Klyatskaya, M. Ruben, and W. Wernsdorfer, Electrically driven nuclear spin resonance in single-molecule magnets, Science **344**, 1135 (2014).
[32] A. J. Sigillito, A. M. Tyryshkin, T. Schenkel, A. A. Houck, and S. A. Lyon, All-electric control of donor nuclear spin qubits in silicon, Nat. Nanotechnol. **12**, 958 (2017).
[33] G. Wolfowicz, M. Urdampilleta, M. L. W. Thewalt, H. Riemann, N. V. Abrosimov, P. Becker, H.-J. Pohl, and J. J. L. Morton, Conditional control of donor nuclear spins in silicon using stark shifts, Phys. Rev. Lett. **113**, 157601 (2014).
[34] J. Liu, J. Mrozek, A. Ullah, Y. Duan, J. J. Baldoví, E. Coronado, A. Gaita-Ariño, and A. Ardavan, Quantum coherent spin–electric control in a molecular nanomagnet at clock transitions, Nat. Phys. **17**, 1205 (2021).
[35] A. Chiesa, E. Macaluso, F. Petiziol, S. Wimberger, P. Santini, and S. Carretta, Molecular nanomagnets as qubits with embedded quantum-error correction, J. Phys. Chem. Lett. **11**, 8610 (2020).
[36] S. J. Lockyer, A. Chiesa, G. A. Timco, E. J. McInnes, T. S. Bennett, I. J. Vitorica-Yrezebal, S. Carretta, and R. E. Winpenny, Targeting molecular quantum memory with embedded error correction, Chem. Sci. **12**, 9104 (2021).
[37] S. Carretta, D. Zueco, A. Chiesa, Á. Gómez-León, and F. Luis, A perspective on scaling up quantum computation with molecular spins, Appl. Phys. Lett. **118**, 240501 (2021).
[38] J. A. Gross, Designing codes around interactions: The case of a spin, Phys. Rev. Lett. **127**, 010504 (2021).
[39] M. Atzori, E. Garlatti, G. Allodi, S. Chicco, A. Chiesa, A. Albino, R. De Renzi, E. Salvadori, M. Chiesa, S. Carretta, and L. Sorace, Radio frequency to microwave coherent manipulation of an organometallic electronic spin qubit coupled to a nuclear qudit, Inorg. Chem. **60**, 11273 (2021).
[40] S. Asaad, V. Mourik, B. Joecker, M. A. I. Johnson, A. D. Baczewski, H. R. Firgau, M. T. Madzik, V. Schmitt, J. J. Pla, F. E. Hudson, K. M. Itoh, J. C. McCallum, A. S. Dzurak, A. Laucht, and A. Morello, Coherent electrical control of a single high-spin nucleus in silicon, Nature (London) **579**, 205 (2020).
[41] B. E. Kane, A silicon-based nuclear spin quantum computer, Nature (London) **393**, 133 (1998).
[42] M. H. Abobeih, J. Cramer, M. A. Bakker, N. Kalb, M. Markham, D. J. Twitchen, and T. H. Taminiau, One-second coherence for a single electron spin coupled to a multi-qubit nuclear-spin environment, Nat. Commun. **9**, 2552 (2018).
[43] E. Moreno-Pineda, C. Godfrin, F. Balestro, W. Wernsdorfer, and M. Ruben, Molecular spin qudits for quantum algorithms, Chem. Soc. Rev. **47**, 501 (2018).
[44] R. Hussain, G. Allodi, A. Chiesa, E. Garlatti, D. Mitcov, A. Konstantatos, K. S. Pedersen, R. De Renzi, S. Piligkos, and S. Carretta, Coherent manipulation of a molecular Ln-based nuclear qudit coupled to an electron qubit, J. Am. Chem. Soc. **140**, 9814 (2018).
[45] R. E. George, W. Witzel, H. Riemann, N. Abrosimov, N. Nötzel, M. L. Thewalt, and J. J. Morton, Electron spin coherence and electron nuclear double resonance of Bi donors in natural Si, Phys. Rev. Lett. **105**, 067601 (2010).
[46] D. A. Golter and H. Wang, Optically driven Rabi oscillations and adiabatic passage of single electron spins in diamond, Phys. Rev. Lett. **112**, 116403 (2014).
[47] G. Balasubramanian, P. Neumann, D. Twitchen, M. Markham, R. Kolesov, N. Mizuochi, J. Isoya, J. Achard, J. Beck, J. Tissler, V. Jacques, P. R. Hemmer, F. Jelezko, and J. Wrachtrup, Ultralong spin coherence time in isotopically engineered diamond, Nat. Mater. **8**, 383 (2009).
[48] A. M. Tyryshkin, S. Tojo, J. J. Morton, H. Riemann, N. V. Abrosimov, P. Becker, H.-J. Pohl, T. Schenkel, M. L. Thewalt, K. M. Itoh, and S. A. Lyon, Electron spin coherence exceeding seconds in high-purity silicon, Nat. Mater. **11**, 143 (2012).
[49] D. Gottesman, Class of quantum error-correcting codes saturating the quantum hamming bound, Phys. Rev. A **54**, 1862 (1996).
[50] S. D. Bartlett, H. de Guise, and B. C. Sanders, Quantum encodings in spin systems and harmonic oscillators, Phys. Rev. A **65**, 052316 (2002).
[51] A. M. Tyryshkin, S. A. Lyon, A. V. Astashkin, and A. M. Raitsimring, Electron spin relaxation times of phosphorus donors in silicon, Phys. Rev. B **68**, 193207 (2003).
[52] C. J. Wedge, G. A. Timco, E. T. Spielberg, R. E. George, F. Tuna, S. Rigby, E. J. L. McInnes, R. E. P. Winpenny, S. J. Blundell, and A. Ardavan, Chemical engineering of molecular qubits, Phys. Rev. Lett. **108**, 107204 (2012).